ACS Catalysis
Letter
pubs.acs.org/acscatalysis

Cu Sub-Nanoparticles on Cu/CeO$_2$ as an Effective Catalyst for Methanol Synthesis from Organic Carbonate by Hydrogenation

Masazumi Tamura,* Takahisa Kitanaka, Yoshinao Nakagawa, and Keiichi Tomishige*

Graduate School of Engineering, Tohoku University, Aoba 6-6-07, Aramaki, Aoba-ku, Sendai 980-8579, Japan

Ⓢ *Supporting Information*

ABSTRACT: Cu/CeO$_2$ works as an effective heterogeneous catalyst for hydrogenation of dimethyl carbonate to methanol at 433 K and even at low H_2 pressure of 2.5 MPa, and it provided 94% and 98% methanol yield based on the carbonyl and total produced methanol, respectively. This is the first report of high yield synthesis of methanol from DMC by hydrogenation with H_2 over heterogeneous catalysts. Characterization of the Cu/CeO$_2$ catalyst demonstrated that reduction of Cu/CeO$_2$ produced Cu metal with <1.0 nm (subnanoparticles). Cu metal subnanoparticles are easily formed by the interaction with the CeO$_2$ surface, which is responsible for the high catalytic performance.

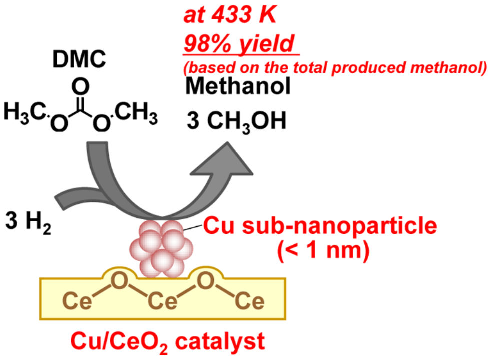

KEYWORDS: *Cu subnanoparticle, Cu/CeO$_2$, hydrogenation, methanol synthesis, organic carbonate*

CO$_2$ can be regarded as an inexpensive, abundant, nontoxic, and renewable resource, and development of efficient methods to transform CO$_2$ to valuable chemicals is promising for constitution of a carbon neutral process. Various target chemicals such as formic acid, methanol, carbonates, and ureas are known[1] and among these target chemicals, methanol has attracted much attention because methanol is used in the production of various useful chemicals such as formaldehyde, dimethyl ether, methyl *tert*-butyl ether, and acetic acid and is expected to be one of the most effective hydrogen carriers in the future.[2]

Methanol is industrially prepared by hydrogenation of CO and CO$_2$ with H_2, where Cu–Zn-based catalysts are known as the most effective catalysts.[3] The reaction generally requires severe conditions such as high temperature (typically 523–573 K) and pressure (typically 5–10 MPa).[1b,3] High temperature is not preferable in terms of the reaction equilibrium and endothermic reverse water–gas shift reaction, bringing about a decrease of the selectivity.[4] Recently, Urakawa et al. achieved excellent selectivity (>98%) at high conversion (>95%) using coprecipitated Cu/ZnO/A$_2$O$_3$ at high pressure (36 MPa) and also reported quite high activity with commercial Cu/ZnO/A$_2$O$_3$.[4l] The activity is the highest among the reported Cu-based catalysts (Table S1). However, the severe reaction conditions (high pressure and high temperature) are a serious problem. On the other hand, effective homogeneous catalysts at low temperature like Ru complexes[5] or effective heterogeneous catalysts at low H_2 pressure (0.05 MPa) like MnO$_x$/m-Co$_3$O$_4$ (<433 K)[6] were reported. However, these catalytic processes also have some drawbacks such as low activity, low yield, and/or high temperature (>473 K).

Recently, Milstein and co-workers proposed a new process for methanol synthesis from CO$_2$, which is an indirect one via hydrogenation of carbonate derivatives such as carbonates, carbamates, and ureas (Scheme 1),[7] because these carbonate derivatives can be comparatively easily synthesized from CO$_2$ by nonreductive transformation. Ru-based homogeneous catalysts are effective for hydrogenation of the carbonyl moiety in these chemicals to methanol at low temperature of 383 K,[7] suggesting the possibility for low-temperature synthesis of methanol. Other researchers also reported on Ru complexes for hydrogenation of cyclic carbonates to methanol and diols.[8] Heterogeneous catalysts are favorable from the viewpoints of green sustainable chemistry. Cu-based heterogeneous catalysts[9] such as CuCr$_2$O$_4$,[9a] Cu/mesoporous-silica,[9b] and Cu-SiO$_2$ nanocomposite[9c] were reported to be efficient for hydrogenation of ethylene carbonate to methanol and ethylene

Scheme 1. Indirect Conversion of CO$_2$ to Methanol by Carboxylation of Methanol with CO$_2$ to DMC and Hydrogenation of DMC to Methanol

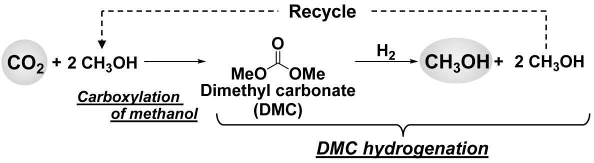

Received: October 8, 2015
Revised: December 1, 2015

DOI: 10.1021/acscatal.5b02258
ACS Catal. 2016, 6, 376–380

Table 1. Effect of Cu Amount over Cu(x)/CeO_2 Catalyst in Hydrogenation of Dimethyl Carbonate (DMC)[a]

			selectivity[b] (%)					
x	conv. (%)	yield (%)	CH_3OH	$HCOOCH_3$	CH_4	CO	CO_2	CH_3OH/Cu[c] (mol/mol)
0	1.2	1.0	82.3	11.9	0.0	0.8	5.0	-
0.1	2.1	1.0	48.7	24.3	0.8	2.2	24.1	99
0.5	5.4	3.4	63.0	23.3	1.0	1.5	11.2	129
1	10.6	8.6	80.8	12.1	1.0	0.9	5.2	164
2	15.4	13.0	84.5	7.8	1.3	1.3	5.4	125
3	13.5	11.0	81.7	8.6	1.6	1.6	6.7	70
5	14.4	11.8	82.0	8.0	1.7	1.7	7.1	45

[a] Reaction conditions: DMC 30 mmol, Cu(x)/CeO_2 100 mg (x = 0−5), THF 5 g, H_2 8 MPa, 433 K, 4 h. [b] Selectivity based on the carbonyl of DMC. [c] CH_3OH/Cu ratio (mol/mol) = (Produced methanol amount based on the carbonyl (mmol))/(Total Cu amount (mmol)).

glycol, where the size of Cu metal particles is comparatively large (≥8 nm) and both Cu^0 and Cu^+ were proposed as the active site (Table S2). However, these catalysts have drawbacks such as low selectivity (<80%), high temperature (453 K), low turnover frequency (TOF < 3 h^{-1}), and/or low turnover number (TON < 10) (Table S2). In addition, the Cu-SiO_2 nanocomposite showed low selectivity and activity in hydrogenation of DMC to methanol,[9c] which was explained by the lower reactivity of linear carbonates than cyclic carbonates (Table S2).[8b,9c] It is essential to develop the effective catalysts with high activity under mild reaction conditions.

Transition metal subnanoclusters, particularly Ag or Au subnanocluster, have attracted much attention in the field of catalysis due to the unique catalytic feature,[10] and Cu subnanocluster is also predicted as a promising unique catalyst by DFT calculations.[11] However, in hydrogenation of CO_2, a large Cu loading amount is generally used for the reaction, and a large particle of Cu metal species is formed (≥3 nm) (Table S1); subnanoparticles of Cu metal species (<1 nm) have not been applied to the reaction. Recently, Curtiss and co-workers first reported that the heterogeneous Cu_4 cluster on Al_2O_3 is effective for hydrogenation of CO_2 at low CO_2 pressure (0.013 MPa) based on the experimental and theoretical results.[12] However, the preparation method of the Cu_4 clusters is very specific and cumbersome. Therefore, development of an easy preparation method of such Cu subnanoparticles will enable a wide range of applications of Cu subnanoparticles.

We have developed CeO_2-catalyzed organic reactions including transformation of CO_2 or nitriles,[13,14] and we have demonstrated that CeO_2 can readily activate CO_2 or esters on the surface of CeO_2.[13] Recently, we reported that the combination catalyst of CeO_2 and 2-cyanopyridine is effective for the synthesis of DMC from CO_2 and methanol to give 94% DMC yield based on methanol at mild reaction temperature of 393 K, which can be related to more environmentally benign and economical synthesis of DMC from CO_2.[14] Considering the reversibility of DMC formation from CO_2 and methanol, introduction of transition metal species for activation of H_2 onto the CeO_2 surface without losing the property of CeO_2 will enable the transformation of DMC to methanol at low temperature. Herein, we report that Cu/CeO_2 is an effective catalyst for hydrogenation of DMC to methanol, providing high methanol yield. Characterization of Cu/CeO_2 catalyst reveals that Cu species on CeO_2 are metallic Cu subnanoparticles.

At first, the catalytic activity for hydrogenation of dimethyl carbonate (DMC) to methanol at 433 K and 8 MPa H_2 was investigated with CeO_2-supported 1 wt % metal catalysts (M(1)/CeO_2, M═Cu, Pt, Ag, Au, Ir, Ni, Rh, Co, Pd, Ru; prepared by impregnation) and conventional carbon-supported 5 wt % noble metal catalysts (M′(5)/C, M′═Ru, Rh, Pd, Pt) (Table S3). In this reaction, three moles of methanol are produced by hydrogenation from the two moles of the methoxy moiety and one mole of the carbonyl moiety in DMC. To precisely estimate the catalytic performance, the selectivity was calculated on the basis of the carbonyl amount of DMC. The details of the calculation method are described in the Supporting Information. M(1)/CeO_2 catalysts except for Cu(1)/CeO_2 showed low conversion (<3%). Similarly, M′(5)/C catalysts showed low conversion and/or low selectivity. Cu(1)/CeO_2 exhibited high conversion and selectivity to methanol, providing higher yield than other M(1)/CeO_2 catalysts. It should be noted that only CeO_2 provided quite low conversion with comparatively high selectivity (80.8%). Therefore, Cu can be regarded as a suitable metal species over CeO_2 in this reaction. Next, effect of supports was also investigated in the same reaction using metal oxides such as ZrO_2, MgO, TiO_2, γ-Al_2O_3, SiO_2−Al_2O_3 (SAL), and SiO_2 as supports (Table S3). Among these metal oxides, CeO_2 showed higher yield and selectivity to methanol than other metal oxides. Therefore, the combination of CeO_2 and Cu is the most effective for the reaction. In addition, Cu(1)/CeO_2 catalyst could be reused without large loss of selectivity and activity (Table S3).

The effect of Cu loading amount was investigated using Cu(x)/CeO_2 catalysts with various amount of Cu (x = 0−5 wt %) (Table 1). The conversion increased with increasing Cu amount from 0 to 2 wt %, but the conversion was almost constant at 2 wt % and larger amount of Cu. On the other hand, the selectivity increased with increasing Cu amount from 0.1 to 1 wt %, and leveled off at more than 1 wt %. The low selectivity at small Cu amount (0.1 and 0.5 wt %) will be due to the low conversion, and alternatively the selectivity to methyl formate, which will be a main intermediate of the reaction, was high. CH_3OH/Cu ratio (mol/mol) provided a volcano pattern with respect to the Cu amount, and the highest CH_3OH/Cu ratio was obtained at 1 wt % Cu amount (Cu(1)/CeO_2). The formation of large Cu metal particle was observed at 5 wt % Cu loaded CeO_2 catalyst (Cu(5)/CeO_2) by XRD analysis (Figure S1), although a part of Cu metal species forms large metal particles in consideration of the peak intensity of Cu metal. This result at least implies that the large Cu particle is unfavorable for the reaction. From the viewpoints of selectivity and activity, Cu(1)/CeO_2 was selected as the optimal catalyst.

Figure 1 shows the time-course of hydrogenation of DMC to methanol over Cu(1)/CeO_2 catalyst (details are shown in Table S4). The reaction proceeded smoothly to reach 100% conversion after 24 h, resulting in the high methanol yield of 94% and 98% based on the carbonyl of DMC and total

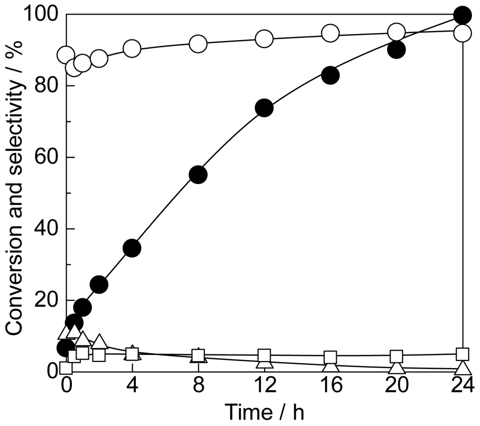

Figure 1. Time-course of hydrogenation of DMC over Cu/CeO_2 catalyst (●: conversion, ○: methanol selectivity, △: methyl formate selectivity, □: others). Selectivity to methanol was calculated on the basis of the carbonyl of DMC. Others include CO, CO_2, and CH_4. Reaction conditions: DMC 15 mmol, Cu(1)/CeO_2 400 mg, THF 5 g, H_2 8 MPa, 433 K.

produced methanol, respectively, and the TON based on total Cu amount reached 224 and 701 based on the carbonyl and total produced methanol, respectively. The number of the TON based on total Cu amount is more than 20 times higher than those in the previous reports on the hydrogenation of carbonates using Cu-based catalysts (Table S2). The selectivity to methanol based on the carbonyl of DMC was high throughout the reaction and gradually increased from 85% to 95%. At the initial stage, formation of methyl formate was observed, and the selectivity gradually decreased with the reaction time, implying that the reaction proceeds via two consecutive reactions: (i) hydrogenation of DMC to methyl formate and (ii) hydrogenation of the methyl formate.

Effect of H_2 pressure was investigated with Cu(1)/CeO_2 in the range of 2.5−9.5 MPa (Table S5). Dependence of H_2 pressure on the conversion and selectivity is very low, although the conversion and selectivity gradually decreased with decreasing H_2 pressure, indicating that operation at low H_2 pressure will be possible with Cu(1)/CeO_2 catalyst. This dependence of H_2 pressure on Cu(1)/CeO_2 is quite different from that over Cu-based catalysts used in hydrogenation of CO_2, where the conversion largely depended on the H_2 pressure.[15] This means that the coverage of the active hydrogen species will be high on Cu/CeO_2. In order to estimate the methanol formation rate (mmol g_{-Cu}^{-1} h^{-1}) and TOF (h^{-1}) based on the carbonyl of DMC and total Cu metal, the time-courses at 8 and 2.5 MPa H_2 were examined below 15% conversion of DMC (Figure S2). From the slope of the time-course, the methanol formation rate (TOF) was calculated to be 417 mmol g_{-Cu}^{-1} h^{-1} (26.5 h^{-1}) and 323 mmol g_{-Cu}^{-1} h^{-1} (20.5 h^{-1}) at 8 and 2.5 MPa H_2, respectively. The activity of Cu(1)/CeO_2 is about 90 times higher than that of the reported Cu-SiO_2 nanocomposite for hydrogenation of DMC (Table S2). In addition, the reaction rate is more than 2 orders of magnitude higher than those of previously reported Cu-based catalysts for hydrogenation of CO_2 to methanol at similar temperature (433 and 453 K), and moreover, the reaction rate is similar to or higher than that at much higher temperature of >523 K (Table S1).

In addition, the hydrogenation of diethyl carbonate (DEC) was also carried out under similar reaction conditions, showing 85% conversion of DEC with 98% selectivity to methanol based on the carbonyl and 98% selectivity to ethanol (Scheme 2). On the other hand, hydrogenation of CO_2 showed no product (Scheme 3). This behavior supports that Cu(1)/CeO_2 is effective specifically for hydrogenation of DMC and DEC.

Scheme 2. Hydrogenation of Diethyl Carbonate (DEC) over Cu(1)/CeO_2[a]

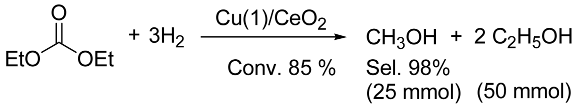

[a] Reaction Conditions: DEC 30 mmol, Cu(1)/CeO_2 1 g, THF 5 g, H_2 8 MPa, 433 K, 48 h.

Scheme 3. Hydrogenation of CO_2 over Cu(1)/CeO_2[a]

$$CO_2 + 3H_2 \xrightarrow{Cu(1)/CeO_2} CH_3OH + H_2O$$

<0.1 mmol

[a] Reaction Conditions: Cu(1)/CeO_2 0.2 g, 1,4-dioxane 20 g, CO_2 2 MPa, H_2 6 MPa, 433 K, 16 h.

To clarify the state of Cu and CeO_2 in Cu(1)/CeO_2 catalyst, Cu(x)/CeO_2 catalysts (x = 0−5) were characterized by XRD, TEM, TPR and XAFS. No Cu species such as CuO, Cu_2O or Cu metal in Cu(1)/CeO_2 after the reaction were observed by XRD and TEM analyses (Figures S1 and S3), which indicates that the size of Cu species are very small. Considering the detection limit of particles by TEM analysis, the size of Cu species will be smaller than 1 nm. In situ XANES and EXAFS measurements were conducted in order to determine the state of Cu species. Figure 2a shows Cu *K*-edge XANES spectra of Cu(1)/CeO_2 reduced under H_2 flow at 433 K and standard Cu samples, which are known to be significantly influenced by the oxidation state and local symmetry of Cu species.[16] The XANES spectrum of the Cu(1)/CeO_2 is quite similar to that of Cu foil. The first derivatives of the XANES spectra were studied to clarify the difference of the spectra (Figure 2b). The peaks are due to the edge energy for each Cu compounds (Cu^0: 8978 eV, Cu^+: 8980 eV, Cu^{2+}: 8982 eV);[16a] the main peak of the Cu(1)/CeO_2 agreed well with that of Cu foil, and the peaks due to Cu^{2+} and Cu^+ were not observed. These results indicate that Cu species in Cu(1)/CeO_2 catalyst after reduction is in the metallic state. In addition, Fourier transform of k^3-weighted Cu *K*-edge EXAFS of the Cu(1)/CeO_2 showed the signal corresponding to the Cu metal (Figure 2c), and the curve-fitting analysis provided the presence of Cu−Cu bond with a coordination number (CN) of 5.5 (Figure 2d and Table S6), which is in good accordance with the result that Cu was in the metallic state by XANES analysis. This CN value is much smaller than the CN of bulk Cu metal (CN = 12), which can be supported by the result that Cu species cannot be observed by XRD and TEM analyses. Based on the CN of the Cu−Cu bonds, the size of Cu metal particle will be at subnanometer scale (<1 nm). TPR analyses of Cu(*x*)/CeO_2 and Cu(1)/SiO_2 catalysts (Figure S4 and Table S7) showed the shift of H_2 consumption signal to lower temperature (473−493 K) by addition of Cu species on CeO_2 compared with the main signal (580 K) of Cu/SiO_2, suggesting that CeO_2 facilitates the reduction of CuO_x species. In addition, the amount of H_2 consumption calculated by the area of the main signal was

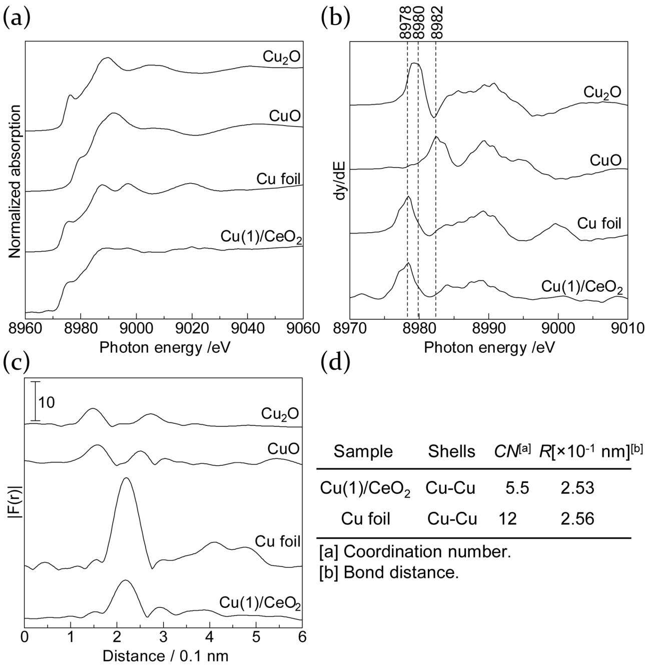

Sample	Shells	CN[a]	R[×10^{-1} nm][b]
Cu(1)/CeO$_2$	Cu-Cu	5.5	2.53
Cu foil	Cu-Cu	12	2.56

[a] Coordination number.
[b] Bond distance.

Figure 2. (a) Cu *K*-edge XANES spectra, (b) first derivatives of XANES spectra ,and (c) Fourier transform of k^3-weighted Cu *K*-edge EXAFS for Cu(1)/CeO$_2$ after reduction and Cu foil, CuO, and Cu$_2$O as references, FT range 30−120 nm^{-1}. (d) Curve-fitting results of Cu *K*-edge of Cu(1)/CeO$_2$ after reduction. (The detailed data were shown in Table S7 and Figure S5.) Reduction conditions: 100% H$_2$ flow, 433 K.

much larger than the loading amount of Cu (Table S7), indicating that Cu species was reduced to Cu metal and that a part of CeO$_2$ was reduced (Ce^{4+} → Ce^{3+}). Compared with the signal of CeO$_2$, the signals of Cu(x)/CeO$_2$ were shifted to lower temperature, indicating that Cu species promote the reduction of CeO$_2$. From these results, Cu species and CeO$_2$ were strongly interacted, leading to promotion of reduction of both CeO$_2$ and CuO$_x$ species. According to the previous works about Cu-supported CeO$_2$ catalysts in wet oxidation of phenol or gas shift reaction,[17] CuO$_x$ species were easily highly dispersed on CeO$_2$ by the strong interaction between CeO$_2$ and Cu ion. This good affinity of Cu ion with CeO$_2$ will be related to the formation of Cu metal subnanoparticles. As above, we first disclosed that Cu subnanoparticles can be easily formed on CeO$_2$ by H$_2$ reduction owing to the strong interaction between Cu species and CeO$_2$. To confirm the stability of the Cu metal subnanoparticles, XRD patterns and XAFS before and after the reaction were compared (Figures S5−7), which provided similar results. Taking the reusability of Cu(1)/CeO$_2$ catalyst into consideration (Table S3), Cu metal subnanoparticles are stable under the reaction conditions. This catalyst is quite different from the reported Cu-based catalysts in hydrogenation of carbonates in terms of the particle size of Cu and the active species.[9] In particular, both Cu^0 and Cu$^+$ can be active species in the reported catalysts; in contrast, the Cu metal subnanoparticles are responsible for this high catalytic performance.

To discuss the mechanism over Cu subnanoparticles, kinetic parameters of H$_2$ pressure and DMC concentration were investigated. The reaction orders with respect to H$_2$ pressure and DMC concentration were calculated to be 0.1 and 0.2, respectively (Figure S8). These results indicate that H$_2$ pressure and DMC concentration hardly influence the reaction rate. The two reaction mechanisms for hydrogenation of CO$_2$ over Cu-based catalysts have been proposed (Scheme 4a): (i) hydrogenation of CO$_2$ to formate adspecies and successive hydrogenation of the formate adspecies, and the latter step is a rate-determining step; (ii) hydrogenation of CO$_2$ to carboxyl adspecies (OCOH) and decomposition of the carboxyl adspecies to CO and OH, and the former step will be a rate-determining step.[4m] In general, the reaction rate in hydrogenation of CO$_2$ strongly depends on the H$_2$ pressure over Cu-based catalysts.[15] On the other hand, the hydrogenation of DMC will proceed through adsorption of molecular DMC instead of the carbonate formation and successive hydrogenation of the molecular DMC (Scheme 4b). The rate-determining step will be the hydrogenation of the molecular DMC adspecies. The molecular DMC adspecies is more reactive than the formate adspecies or CO$_2$ from the viewpoint of the electronic density of the carbonyl group, so that the hydrogenation of DMC will proceed at lower reaction temperature than hydrogenation of CO$_2$. In addition, no activity for hydrogenation CO$_2$ over Cu(1)/CeO$_2$ suggests that Cu(1)/CeO$_2$ is especially effective for DMC hydrogenation. The higher activity of Cu subnanoparticles than those of reported Cu-SiO$_2$ in hydrogenation of DMC (>90-fold, Table S2) indicates that the particle size of Cu metal is largely connected to the reaction rate. Considering the zero reaction orders with respect to the H$_2$ pressure and DMC concentration, adsorption of DMC and dissociation of H$_2$ will be very fast, and the adspecies of DMC and hydrogen will be saturated on the Cu particles. Therefore, the active hydrogen species can be produced on Cu subnanoparticles, which leads to the high activity of Cu-nanoparticles on Cu(1)/CeO$_2$ in the hydrogenation of DMC.

Scheme 4. Typical Mechanism of Hydrogenation of CO$_2$ over Cu-Based Catalysts (a) and Proposed Mechanism of DMC over Cu Metal Particles (b)

(a) Typical mechanism for hydrogenation of CO$_2$ over Cu-based catalysts

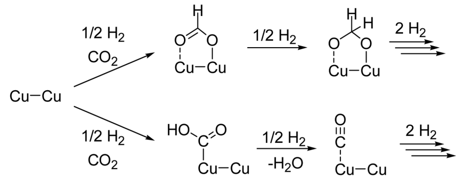

(b) Proposed mechanism for hydrogenation of DMC

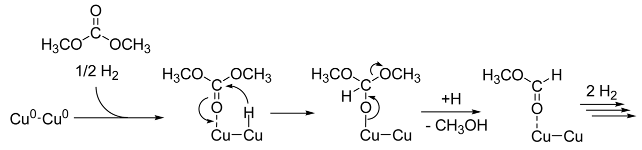

In summary, we have demonstrated that Cu/CeO$_2$ is an effective heterogeneous catalyst for hydrogenation of DMC to methanol at the low reaction temperature of 433 K and even at low H$_2$ pressure of 2.5 MPa. The methanol yield reached 94% and 98% based on the carbonyl of DMC and total produced methanol, respectively, and the TON based on total Cu metal was 224 and 701 based on the carbonyl and total produced methanol, respectively, which are 2 orders of magnitude higher than those in the previous reports. The activity of Cu(1)/CeO$_2$ in this reaction is also pretty high, and the methanol formation rate is much higher than the typical Cu-based catalysts for hydrogenation of CO_2 (more than 2 orders of magnitude at comparable reaction temperature and pressure). Various analyses such as XAFS, XRD, TEM, and TPR showed that Cu species on Cu(1)/CeO_2 were reduced to Cu metal and that the size of Cu metal is below 1 nm (Cu subnanoparticles). We can conclude that heterogeneous Cu metal subnanoparticles can be easily formed on CeO_2, exhibiting the high catalytic performance for hydrogenation of DMC.

■ ASSOCIATED CONTENT

Supporting Information

The Supporting Information is available free of charge on the ACS Publications website at DOI: 10.1021/acscatal.5b02258.

> Experimental details of the catalyst preparation, reaction and catalyst characterization, and the details of results (XRD, TEM, TPR, XAFS, kinetics, and GC-chart) (PDF)

■ AUTHOR INFORMATION

Corresponding Authors

*E-mail: mtamura@erec.che.tohoku.ac.jp.
*E-mail: tomi@erec.che.tohoku.ac.jp.

Notes

The authors declare no competing financial interest.

■ REFERENCES

(1) (a) Mikkelsen, M.; Jørgensen, M.; Krebs, F. C. *Energy Environ. Sci.* **2010**, *3*, 43−81. (b) Sakakura, T.; Choi, J.-C.; Yasuda, H. *Chem. Rev.* **2007**, *107*, 2365−2387. (c) Liu, Q.; Wu, L.; Jackstell, R.; Beller, M. *Nat. Commun.* **2015**, *6*, 5933.

(2) (a) Olah, G. A.; Goeppert, A.; Prakash, G. K. S. *Beyond Oil and Gas: The Methanol Economy*; Wiley-VCH: Weiheim, 2009. (b) Olah, G. A. *Angew. Chem., Int. Ed.* **2005**, *44*, 2636−2639.

(3) (a) Behrens, M.; Studt, F.; Kasatkin, I.; Kühl, S.; Hävecker, M.; Abild-Pedersen, F.; Zander, S.; Girgsdies, F.; Kurr, P.; Kniep, B. L.; Tovar, M.; Fischer, R. W.; Nørskov, J. K.; Schlögl, R. *Science* **2012**, *336*, 893−897. (b) Wang, W.; Wang, S.; Ma, X.; Gong, J. *Chem. Soc. Rev.* **2011**, *40*, 3703−3727.

(4) (a) Liu, J.; Shi, J.; He, D.; Zhang, Q.; Wu, X.; Liang, Y.; Zhu, Q. *Appl. Catal., A* **2001**, *218*, 113−119. (b) Toyir, J.; Ramírez de la Piscina, P.; Fierro, J. L. G.; Homs, N. *Appl. Catal., B* **2001**, *34*, 255−266. (c) Toyir, J.; Ramírez de la Piscina, P.; Fierro, J. L. G.; Homs, N. *Appl. Catal., B* **2001**, *29*, 207−215. (d) Słoczyński, J.; Grabowski, R.; Kozłowska, A.; Olszewski, P.; Stoch, J.; Skrzypek, J.; Lachowska, M. *Appl. Catal., A* **2004**, *278*, 11−23. (e) Liu, X.-M.; Lu, G. Q.; Yan, Z.-F. *Appl. Catal., A* **2005**, *279*, 241−245. (f) Słoczyński, J.; Grabowski, R.; Olszewski, P.; Kozłowska, A.; Stoch, J.; Lachowska, M.; Skrzypek, J. *Appl. Catal., A* **2006**, *310*, 127−137. (g) Raudaskoski, R.; Niemela, M. V.; Keiski, R. L. *Top. Catal.* **2007**, *45*, 57−60. (h) Guo, X.; Mao, D.; Wang, S.; Wu, G.; Lu, G. *Catal. Commun.* **2009**, *10*, 1661−1664. (i) Guo, X.; Mao, D.; Lu, G.; Wang, S.; Wu, G. *J. Catal.* **2010**, *271*, 178−185. (j) An, X.; Li, J.; Zuo, Y.; Zhang, Q.; Wang, D.; Wang, J. *Catal. Lett.* **2007**, *118*, 264−269. (k) Karelovic, A.; Ruiz, P. *Catal. Sci. Technol.* **2015**, *5*, 869−881. (l) Bansoda, A.; Urakawa, A. *J. Catal.* **2014**, *309*, 66−70. (m) Graciani, J.; Mudiyanselage, K.; Xu, F.; Baber, A. E.; Evans, J.; Senanayake, S. D.; Stacchiola, D. J.; Liu, P.; Hrbek, J.; Fernández Sanz, J.; Rodriguez, J. A. *Science* **2014**, *345*, 546−550.

(5) (a) Rezayee, N. M.; Huff, C. A.; Sanford, M. S. *J. Am. Chem. Soc.* **2015**, *137*, 1028−1031. (b) Wesselbaum, S.; vom Stein, T.; Klankermayer, J.; Leitner, W. *Angew. Chem., Int. Ed.* **2012**, *51*, 7499−7502. (c) Huff, C. A.; Sanford, M. S. *J. Am. Chem. Soc.* **2011**, *133*, 18122−18125.

(6) Li, C. S.; Melaet, G.; Ralston, W. T.; An, K.; Brooks, C.; Ye, Y.; Liu, Y. Y. S.; Zhu, J.; Guo, J.; Alayoglu, S.; Somorjai, G. A. *Nat. Commun.* **2015**, *6*, 6538.

(7) (a) Balaraman, E.; Gunanathan, C.; Zhang, J.; Shimon, L. J. W.; Milstein, D. *Nat. Chem.* **2011**, *3*, 609−614. (b) Balaraman, E.; Ben-David, Y.; Milstein, D. *Angew. Chem., Int. Ed.* **2011**, *50*, 11702−11705.

(8) (a) Han, Z.; Rong, L.; Wu, J.; Zhang, L.; Wang, Z.; Ding, K. *Angew. Chem., Int. Ed.* **2012**, *51*, 13041−13045. (b) Kim, S. H.; Hong, S. H. *ACS Catal.* **2014**, *4*, 3630−3636. (c) vom Stein, T.; Meuresch, M.; Limper, D.; Schmitz, M.; Hölscher, M.; Coetzee, J.; Cole-Hamilton, D. J.; Klankermayer, J.; Leitner, W. *J. Am. Chem. Soc.* **2014**, *136*, 13217−13225. (d) Wesselbaum, S.; Moha, V.; Meuresch, M.; Brosinski, S.; Thenert, K. M.; Kothe, J.; vom Stein, T.; Englert, U.; Hölscher, M.; Klankermayer, J.; Leitner, W. *Chem. Sci.* **2015**, *6*, 693−704.

(9) (a) Lian, C.; Ren, F.; Liu, Y.; Zhao, G.; Ji, Y.; Rong, H.; Jia, W.; Ma, L.; Lu, H.; Wang, D.; Li, Y. *Chem. Commun.* **2015**, *51*, 1252−1254. (b) Chen, X.; Cui, Y.; Wen, C.; Wang, B.; Dai, W.-L. *Chem. Commun.* **2015**, *51*, 13776−13778. (c) Liu, H.; Huang, Z.; Han, Z.; Ding, K.; Liu, H.; Xia, C.; Chen, J. *Green Chem.* **2015**, *17*, 4281−4290.

(10) (a) Lu, Y.; Chen, W. *Chem. Soc. Rev.* **2012**, *41*, 3594−3623. (b) Taketoshi, A.; Haruta, M. *Chem. Lett.* **2014**, *43*, 380−387. (c) Lei, Y.; Mehmood, F.; Lee, S.; Greeley, J.; Lee, B.; Seifert, S.; Winans, R. E.; Elam, J. W.; Meyer, R. J.; Redfern, P. C.; Teschner, D.; Schlögl, R.; Pellin, M. J.; Curtiss, L. A.; Vajda, S. *Science* **2010**, *328*, 224−228.

(11) (a) Varghese, J. J.; Mushrif, S. H. *J. Chem. Phys.* **2015**, *142*, 184308. (b) Yang, M.; Jackson, K. A.; Koehler, C.; Frauenheim, T.; Jellinek, J. *J. Chem. Phys.* **2006**, *124*, 024308. (c) Guvelioglu, G. H.; Ma, P.; He, X.; Forrey, R. C.; Cheng, H. *Phys. Rev. Lett.* **2005**, *94*, 026103.

(12) Liu, C.; Yang, B.; Tyo, E.; Seifert, S.; DeBartolo, J.; von Issendorff, B.; Zapol, P.; Vajda, S.; Curtiss, L. A. *J. Am. Chem. Soc.* **2015**, *137*, 8676−8679.

(13) (a) Honda, M.; Suzuki, A.; Noorjahan, B.; Fujimoto, K.-i.; Suzuki, K.; Tomishige, K. *Chem. Commun.* **2009**, 4596−4598. (b) Honda, M.; Kuno, S.; Sonehara, S.; Fujimoto, K.-i.; Suzuki, K.; Nakagawa, Y.; Tomishige, K. *ChemCatChem* **2011**, *3*, 365−370. (c) Tamura, M.; Tomishige, K. *Angew. Chem., Int. Ed.* **2015**, *54*, 864−867. (d) Tamura, M.; Wakasugi, H.; Shimizu, K.-i.; Satsuma, A. *Chem. - Eur. J.* **2011**, *17*, 11428−11431. (e) Tamura, M.; Tonomura, T.; Shimizu, K.-i.; Satsuma, A. *Green Chem.* **2012**, *14*, 717−724. (f) Tamura, M.; Honda, M.; Noro, K.; Nakagawa, Y.; Tomishige, K. *J. Catal.* **2013**, *305*, 191−203. (g) Tamura, M.; Siddiki, S. M. A. H.; Shimizu, K.-i. *Green Chem.* **2013**, *15*, 1641−1646. (h) Honda, M.; Tamura, M.; Nakao, K.; Suzuki, K.; Nakagawa, Y.; Tomishige, K. *ACS Catal.* **2014**, *4*, 1893−1896. (i) Tamura, M.; Sawabe, K.; Tomishige, K.; Satsuma, A.; Shimizu, K.-i. *ACS Catal.* **2015**, *5*, 20−26.

(14) (a) Honda, M.; Tamura, M.; Nakagawa, Y.; Sonehara, S.; Suzuki, K.; Fujimoto, K.; Tomishige, K. *ChemSusChem* **2013**, *6*, 1341−1344. (b) Honda, M.; Tamura, M.; Nakagawa, Y.; Nakao, K.; Suzuki, K.; Tomishige, K. *J. Catal.* **2014**, *318*, 95−107.

(15) Bansode, A.; Tidona, B.; von Rhor, P. R.; Urakawa, A. *Catal. Sci. Technol.* **2013**, *3*, 767−778.

(16) (a) Okamoto, Y.; Kubota, T.; Gotoh, H.; Ohto, Y.; Aritani, H.; Tanaka, T.; Yoshida, S. *J. Chem. Soc., Faraday Trans.* **1998**, *94*, 3743−3752. (b) Yamashita, H.; Matsuoka, M.; Tsuji, K.; Shioya, Y.; Anpo, M.; Che, M. *J. Phys. Chem.* **1996**, *100*, 397−402.

(17) (a) Arena, F.; Giovenco, R.; Torre, T.; Venuto, A.; Parmaliana, A. *Appl. Catal., B* **2003**, *45*, 51−62. (b) Hočevar, S.; Krašovec, U. O.; Orel, B.; Aricó, A. S.; Kim, H. *Appl. Catal., B* **2000**, *28*, 113−125. (c) Li, L.; Zhan, Y.; Zheng, Q.; Zheng, Y.; Chen, C.; She, Y.; Lin, X.; Wei, K. *Catal. Lett.* **2009**, *130*, 532−540.